Vertical Seismic Response of a Precast Segmental Bridge Superstructure

M. Anagnostopoulou, A. Filiatrault & A. Aref
Dept. Of Civil, Structural and Environmental Engineering, State University of New York at Buffalo, Buffalo NY, USA

15 WCEE
LISBOA 2012

ABSTRACT
Segmental construction methods using precast concrete are a practical example of Accelerated Bridge Construction (ABC), which can ease costs while maintaining quality. While the popularity of precast concrete segmental bridges has increased throughout the world, their use in seismic regions has been hampered by a lack of understanding of their dynamic response under seismic loads. This paper investigates numerically the vertical non-linear dynamic response of a simple span segmental bridge superstructure that incorporates ABC design concepts. The superstructure segments are stressed together by continuous internal unbonded tendons to ensure the system's enhanced self-centring capability. A series of Incremental Dynamic Analysis (IDA) is conducted by scaling a set of vertical historical earthquake ground motions to different intensity levels. The response of the segmental superstructure bridge system is evaluated by assessing the variability of characteristic response quantities and assigning performance limit states.

Keywords: unbonded tendons; incremental dynamic analysis; non-linear dynamic response; limit states

1. INTRODUCTION

Recent years have witnessed growing interest in Accelerated Bridge Construction (ABC) as an answer to the need for reconstruction of major highways while achieving minimal delay and community disruption. A practical example of ABC incorporates discrete precast elements to form the superstructure and substructure of the bridge, and post-tensioned tendons to act as the continuity reinforcement between adjacent segments. The number of precast segmental bridge applications has increased during the last years but most of them are located in regions of low seismicity. Under seismic loads, precast segmental bridges can dissipate seismic energy through the cyclic opening and closure of the segment-to-segment joints, while exhibiting an enhanced self-centring capability. The dynamic response of precast segmental bridges, in regions of moderate to high seismicity, is therefore believed to result in large vertical deflections, significant residual displacements and joint openings.

This paper presents the results of a numerical study that investigates the response of precast segmental concrete bridge superstructures, designed according to the ABC techniques, when subjected to vertical earthquake loads. Even though the impact of vertical earthquake motion on the segment-joint response has been investigated by a number of research programs and experimental studies, current bridge design codes do not account for the effect of vertical ground motions and provide little guidance on the development of a vertical design spectrum.

In this study a key concept is introduced in the design of the segmental superstructure; namely, the use of internal unbonded post-tensioned tendons acting as the continuous reinforcement between the superstructure's segments. Bonded tendons in precast segmental structures lead to conventional cast-in-place behaviour of the system; whereas unbonded tendons allow the opening and closure of the joints between adjacent segments and therefore, the rocking behaviour of the system. Even though the enhanced self-centring behaviour of post-tensioned precast segmental piers with unbonded tendons has been widely demonstrated (e.g., Ou et al., 2010), the use of internal unbonded tendons in precast segmental bridge superstructures has never been reported in the literature.

2. SEGMENTAL SUPERSTRUCTURE MODEL

2.1 General Description

The prototype bridge structure used for this study is the one considered by Megally et al. (2002). It is a single-cell box girder bridge that consists of five spans with three interior spans of 30.5 m (100 ft) and exterior spans of 22.9 m (75 ft) for a total length of 137.2 m (450 ft). Each span of the prototype structure is post-tensioned with a harped-shape tendon. The segmental superstructure model considered in this study represents the centre span of the prototype bridge with two overhangs. The interior span length is 30.5 m (100 ft) and the length of each overhang is 7.6 m (25 ft) for a total length of 45.7 m (150 ft).

In order to comply with the ABC techniques for precast segmental bridges, the superstructure is divided into segments. A segment-to-segment joint is provided at the mid-span section, where high bending moments and low shear forces are induced. Mid-span is also the location where maximum relative displacement of the segments is expected when the superstructure is subjected to vertical seismic loading. The segmental superstructure consists of six interior segments 6.1 m (20 ft) long and two exterior segments 4.6 m (15 ft) long. The precast segments are match cast, which means that each segment is cast against the previous one so that the end face of one segment is an imprint of the neighbour segment. No shear keys or epoxy adhesives are considered at the joints. The uniform behaviour of the system is achieved through post-tensioning of the segments with internal unbonded tendons (DYWIDAG, 2009).

2.2 Modelling Approach

A two-dimensional numerical model of the segmental superstructure, which incorporates material and geometric nonlinearities, is developed and analyzed using the inelastic dynamic analysis software RUAUMOKO (Carr, 2007). The segments of the superstructure are modelled using linear elastic frame type members except for a region at the ends of each segment which is discretized into several axial non-linear springs. The springs are connected to the ends of the superstructure beam elements through rigid body links.

Prior to loading, a joint between two adjacent segments is closed and the whole section is in compression. When a vertical seismic load is applied, the joint opens and a compressive contact zone forms. In order to accurately simulate the contact zone between adjacent segments, the number and distribution of contact springs shall be selected such that the area and second moment of inertia of the contact springs do not significantly deviate from the area and second moment of inertia of the superstructure's cross-section. The hysteresis rule used to model the contact springs is the bi-linear with slackness hysteresis rule (Carr, 2007). A large initial slackness displacement value is selected to ensure that no tensile forces are developed in the springs.

Based on the geometry of the superstructure's cross-section, the contact zone between two adjacent segments is modelled with eleven nonlinear contact springs, eight of which are located at the top and bottom plate where maximum local deformations are expected. In order to compute the axial stiffness of the contact springs, their length shall be estimated based on the geometric characteristics of the superstructure's cross-section. For this study, the portion of the superstructure's segments modelled by contact springs is assumed to be equal to $h/8$, where h is the depth of the cross-section, thus 23.0 cm (9.0 in) at each end.

The post-tensioning system consists of 80 unbonded mono-strand tendons with a strand diameter equal to 15.2 mm (0.6 in) and an ultimate strength equal to 1860 MPa (270 ksi). In order to minimize the number of numerical elements, the 80 tendons are modelled as a single tendon of equivalent cross-sectional area and parabolic profile. The unbonded tendons are modelled using several bi-linear elastic spring elements in series. More information on the adopted modelling approach can be found in Anagnostopoulou (2009).

Figure 2.1 shows the geometry of the developed segmental superstructure and the corresponding numerical model. The location of the segment-to-segment joints is indicated together with the various structural elements (e.g., concrete segments/frame members, joints/contact spring elements, tendons/spring elements). By performing a modal analysis of the numerical model, the first natural period of the system is found to be 0.305 sec (3.28 Hz) and the second and third natural periods are found to be 0.106 sec (9.42 Hz) and 0.007 sec (14.14 Hz), respectively.

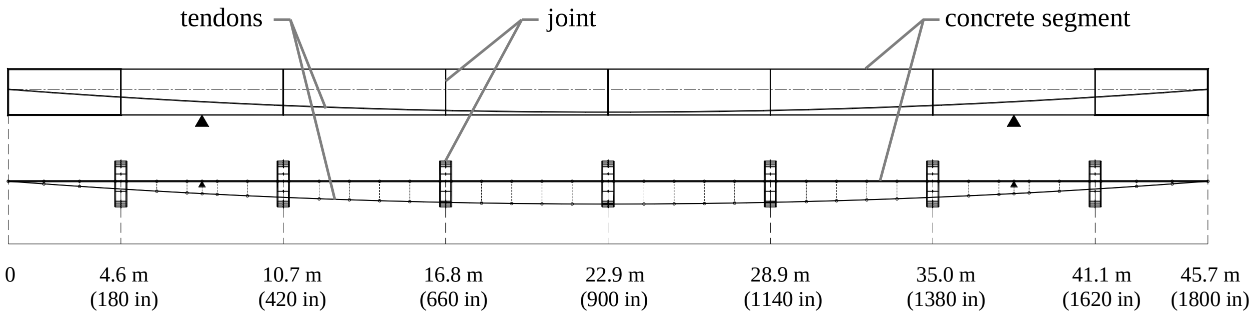

Figure 2.1. Geometry of the one-span segmental bridge superstructure and the developed numerical model

3. INCREMENTAL DYNAMIC ANALYSIS

3.1 Earthquake Excitations

The site location for the bridge model is assumed to be in the Western United States, close to the City of Los Angeles. The design spectrum is selected from the AASHTO LRFD Bridge Design Specifications (2007) and represents a seismic event with a 10% probability of exceedance in 50 years (475-year return period). The acceleration coefficient, A, is assumed to be equal to 0.60 (Seismic Zone 4) and the site coefficient, S, equal to 1.20 (Soil profile type II). Moreover, the Design Earthquake (DE) and Maximum Considered Earthquake (MCE) response spectra are defined according to ASCE/SEI 7-05 (2005). For the specific site location and 5% of critical damping, ASCE specifies the following design and maximum earthquake spectral response acceleration parameters: S_{DS} equals 1.415 g, S_{D1} equals 0.784 g, S_{MS} equals 2.123 g and S_{M1} equals 1.176 g.

The segmental superstructure model is analyzed using the far-field earthquake ground motion ensemble defined in FEMA P-695 (2009). The ensemble consists of twenty-two historical strong ground motions. Initially, a scaling procedure is applied to the horizontal components of the P-695 ground motions: for the DE and MCE intensity levels, the acceleration response spectrum of each record (2×22 = 44 records) is multiplied by a factor defined as the ratio of the DE and MCE spectral accelerations, respectively, at a target period equal to the fundamental period of vibration of the superstructure model, over the geometric mean of the forty four horizontal spectral acceleration values at the same target period. Given that the current bridge design codes provide little guidance on the development of vertical design spectra, the scale factors obtained from scaling the horizontal components of the ground motions are also used for scaling the vertical components of the ground motions to the DE and MCE intensity levels (the vertical component of one record is not available, so 21 records are considered in total). Figure 3.1 shows the results of the scaling method for the horizontal and vertical components of the P-695 ground motions at the DE intensity level.

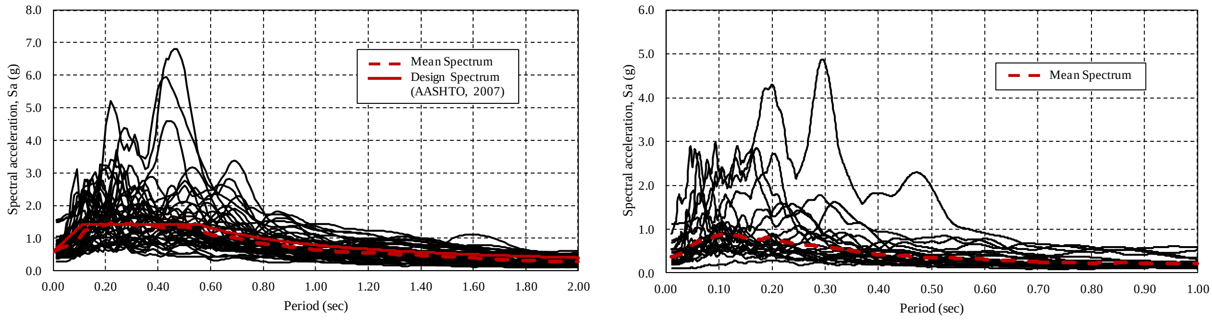

a) Horizontal response spectra b) Vertical response spectra

Figure 3.1. Horizontal and vertical Design acceleration response spectra

3.2 Performance Limit States

The performance limit states of the segmental superstructure can be defined when the numerical model is analyzed under a vertical cyclic sinusoidal displacement-controlled load, which matches the profile of the model's first mode of vibration. Four performance limit states are identified: the onset of joint opening; the cracking of the section; the onset of spalling of the section's extreme concrete fibbers; and either the crushing of the section's confined core or the yielding of the tendons.

The first performance limit state, designated by *PS1*, is associated with the onset of joint opening. According to AASHTO (2007), a segmental superstructure must behave as a monolithic system for the serviceability limit states and allow for joint opening under the ultimate limit states. The allowable compressive concrete stress for pre-stressed components with unbonded tendons at service limit state is equal to $0.60f'_c$ whereas; no tensile stresses shall develop. Considering a concrete compressive strength, f_c', equal to 34.5 MPa (5.0 ksi), the allowable compressive stress is 20.7 MPa (3.0 ksi) and the corresponding concrete stain, ε_c, is 0.07%. In terms of maximum vertical displacement, the AASHTO (2007) specifies a deflection limit equal to $L/800$ under the effect of vehicular loads, where L is the span length of the bridge. For the case of the segmental superstructure model with an interior span length equal to 30.5 m (100 ft), the deflection limit is set equal to 3.8 cm (1.5 in).

The second performance limit state, designated by *PS2*, is associated with the initiation of cracking in the ends of each segment and adjacent to the segment-to-segment joints. The strain level at which cracking of the unconfined concrete occurs is assumed to be equal to 0.12% (AASHTO, 2007). The third performance limit state, designated by *PS3*, is associated with the onset of spalling of the extreme concrete fibbers adjacent to the segment-to-segment joints. The strain level at which the cover concrete ceases to carry any stresses is assumed to be equal to 0.30% (AASHTO, 2007).

The fourth performance limit state, designated by *PS4*, is associated either with the crushing of the confined concrete core or the yielding of the tendons. The strain level at which crashing of the confined concrete occurs is assumed to be equal to 1.0%. The yielding stress of the tendons equals 1675 MPa (243 ksi) which corresponds to a strand strain, ε_{pt}, equal to 0.85%. Table 3.1 summarizes the considered concrete and post-tensioning performance limit states.

Table 3.1. Performance limit states

Perf. State	Description	Displacement/Strain	Consequences
PS1	Onset of joint opening	d = 3.8 cm, ε_c = -0.07%	Inspect, no repair required
PS2	Concrete cracking	ε_c = -0.12%	Inspect, patching of concrete may be required
PS3	Spalling of extreme concrete fibres	ε_c = -0.30%	Patching of concrete, inspect for permanent displacements
PS4	Crushing of concrete core *or* yield of tendons	ε_c = -1.0% *or* ε_{pt} = 0.85%	Repair components, inspect for residual joint openings and displacements

3.3 Analysis Response Parameters

This study focuses on the behaviour of the mid-span joint where maximum relative displacement of the adjacent superstructure segments is expected when the system is subjected to vertical seismic loading. The seismic response of the segmental superstructure is evaluated by examining the variation of characteristic response quantities such as: the maximum upward and downward vertical displacement of the mid-span section; the maximum top and bottom gap opening of the mid-span contact zone (maximum elongation of top and bottom compression springs at mid-span section); the axial stress levels in the unbonded tendons; the residual joint opening of the mid-span joint and; the vertical residual displacement of the mid-span section.

A representative example of the numerical model's response is presented hereafter using as input to the model the Kobe, 1995 ground motion scaled to match the DE intensity level. Figure 3.2 presents the acceleration time history applied to the system, the acceleration response computed at the mid-span joint, the vertical displacement response of the mid-span joint, and the axial deformation response at the top mid-span section. The acceleration time history plots indicate an amplification of the imposed motion at the mid-span of the segmental superstructure, which can be attributed to resonance effects. The maximum downward displacement at mid-span equals 67.3 mm (2.65 in) and is significantly higher than the corresponding maximum upward displacement which equals 20.5 mm (0.81 in). The system's response is characterised by negligible vertical residual displacement and residual joint opening.

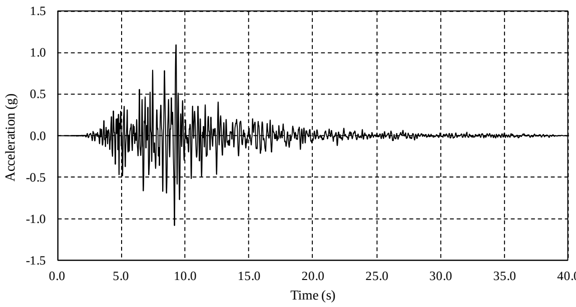

a) Input acceleration time history

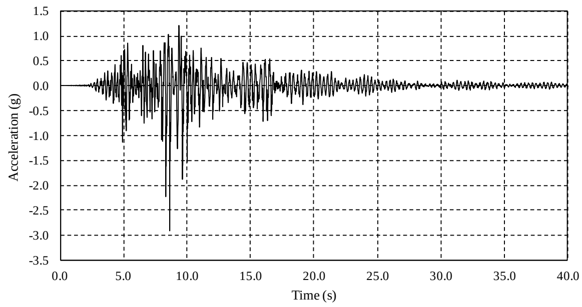

b) Acceleration time history at mid-span

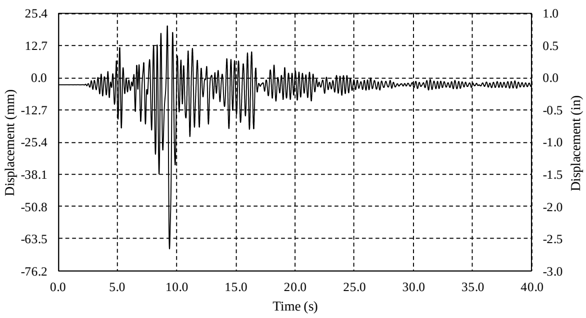

c) Vertical displacement response at mid-span

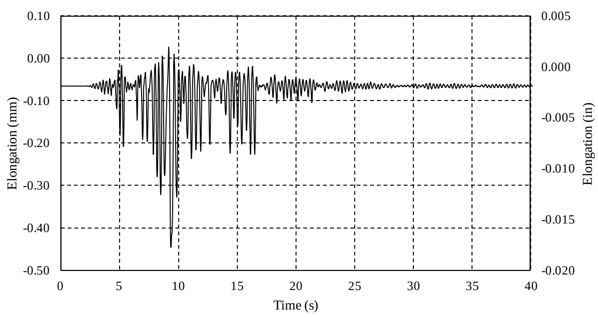

d) Top axial deformation response at mid-span

Figure 3.2. Time history plots for Kobe (1995) record at Design Earthquake level

In addition, the response of the segmental superstructure is explored using the same Kobe, 1995 ground motion scaled to various seismic intensity levels up the MCE event. Table 3.2 summarizes key response results in accordance with the performance limit states defined above. For a maximum downward vertical displacement equal to 3.8 cm (1.5 in) at mid-span defined for *PS1*, the concrete compressive strain at the top of the cross-section reaches a value of 0.07% which corresponds to a joint deformation equal to 0.33 mm (0.013 in). The corresponding values of joint opening at the bottom of the mid-span for *PS1* and *PS2* are approximately equal to 5.18 mm (0.204 in) and 11.94 mm (0.470 in), respectively.

Based on the results presented in Figure 3.2 and Table 3.2, it becomes evident that approximately 55% of the Kobe, 1995 record amplitude-scaled at the DE level can cause *PS1*; whereas the Kobe, 1995 record amplitude-scaled at the MCE level can cause *PS2*. It should be noted that, the values of maximum downward displacement for *PS3* and *PS4* could not be obtained without considering higher seismic intensity levels than the MCE.

Table 3.2. Key response results of mid-span joint due to Kobe, 1995 record

Perf. State	**Displacement** (mm)	**Concrete Strain** (%)	**Joint Deformation** (mm)
PS1	38.1	0.07	0.33
PS2	96.5	0.12	0.56
PS3	N/A	0.30	1.37
PS4	N/A	1.0	4.57

3.4 Seismic Response

Once the numerical model has been developed and the ground motion records have been selected, Incremental Dynamic Analysis (IDA) is performed (Vamvatsikos et al, 2002). To start the analysis, the chosen earthquake records need to be scaled from a low Intensity Measure (IM) to several higher IM levels until either the MCE intensity level is reached or the concrete and pos-tensioning performance limit states are met. For each increment of IM, a nonlinear dynamic time history analysis is performed. The median spectral acceleration at the fundamental vertical period of the segmental superstructure is selected as an appropriate IM for this study.

Locating the maximum values of selected response quantities or Demand Parameters (DP) observed in an analysis gives one point in each of the IM versus DP curve (e.g. S_a vs. vertical displacement at mid-span). By connecting such points obtained from all the analyses using each earthquake record with different IMs gives the IDA curves for all earthquakes in the ensemble.

Two sets of IDA curves for the segmental superstructure numerical model and the suite of twenty one vertical ground motions are presented in Figures 3.3 and 3.4. The DPs are the maximum downward and upward vertical displacements at mid-span of the superstructure. The values of the median spectral acceleration, S_a, at the fundamental vertical period of the segmental superstructure for the DE and MCE intensity levels are indicted in the plots and are equal to 0.59 g and 0.89 g, respectively.

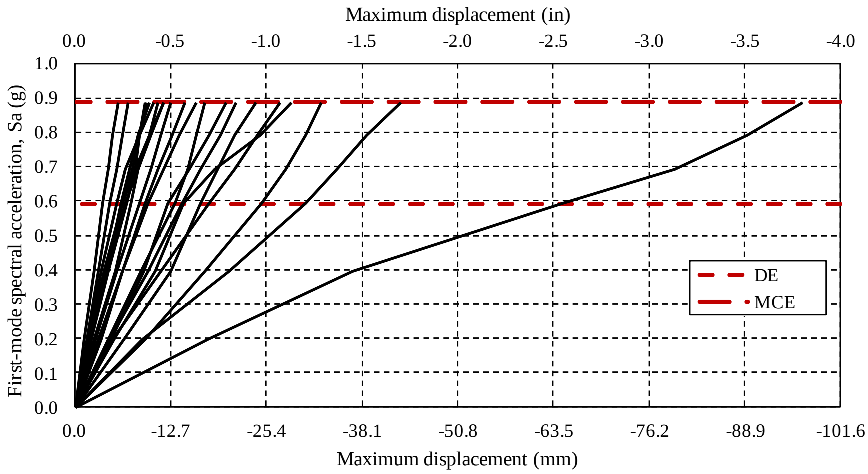

Figure 3.3. IDA curves for maximum downward vertical displacement at mid-span

Figure 3.3 shows that the maximum downward displacement at the superstructure's mid-span ranges from 3.8 mm (0.15 in) to 63.5 mm (2.50 in) for the DE intensity level, and from 5.1 mm (0.20 in) to 96.5 mm (3.80 in) for the MCE intensity level. The minimum response is observed for the El Centro, 1987 record and the maximum response is observed for the Kobe, 1995 record. The majority of the IDAs with the exception of two curves fall below the deflection limit specified for the performance limit state *PS1* which is equal to 38.1 mm (1.50 in). Moreover, none of the IDA curves reach a 'flatline' portion, which is an indication that any increase in the IM results in practically infinite DP response and dynamic instability of the structural system. Given that none of the IDA curves reach the 'flatline', the segmental superstructure system can sustain higher levels of shacking than the MCE without suffering global dynamic instability.

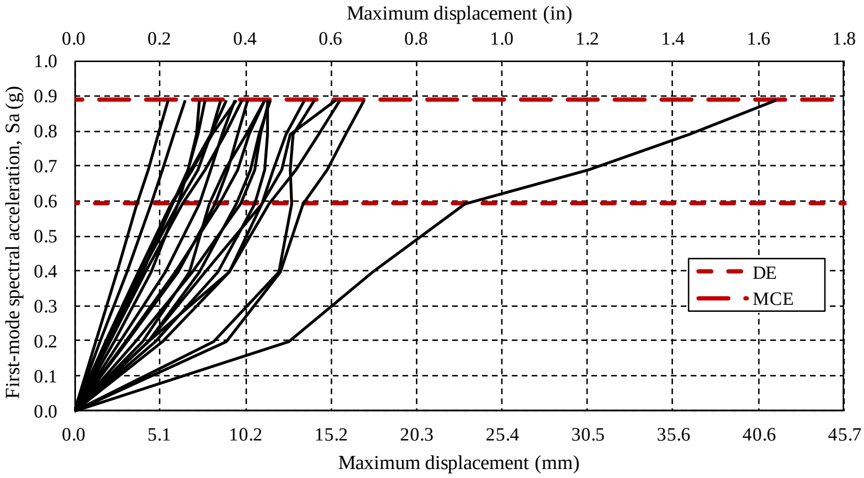

Figure 3.4. IDA curves for maximum upward vertical displacement at mid-span

Figure 3.4 shows that the maximum upward displacement at the superstructure's mid-span ranges from 3.8 mm (0.15 in) to 23.1 mm (0.91 in) for the DE intensity level and from 5.6 mm (0.22 in) to 41.7 mm (1.64 in) for the MCE intensity level. It is evident that the values of upward displacement at the superstructure's mid-span are significantly lower than the corresponding values of downward displacement due to the geometry of the post-tensioning system.

The IDA results are presented hereafter in the form of cumulative probability of non-exceedance plots of the selected analysis response parameters and the two characteristic intensity levels, the DE and MCE events. These plots show the probability that an outcome in the population of the entire set of outcomes of a selected response quantity will have a value that is less than or equal to the specified value x ($0 \leq x \leq 1.0$). The lognormal distribution has been selected as an appropriate form of distribution for all response quantities. The values of the median value, μ, and the standard deviation or dispersion, β, are used to define the lognormal distribution of each response parameter.

Figure 3.5 presents the cumulative probability distribution functions of the maximum downward and upward vertical displacement at mid-span of the segmental superstructure for the DE and MCE intensity levels. Also shown in Figure 3.5 are the two damage state bands described above and listed in Table 3.1.

The response of the segmental superstructure depends on the geometry of the pre-stressing tendons along its length. Given that the unbonded tendons are lying below the model's centre of gravity, it is reasonable that the maximum downward vertical displacement is greater than the maximum upward vertical displacement for a fixed probability and intensity level. The maximum downward vertical displacement band of 38.1 mm (1.50 in) defined for *PS1* is exceeded by one record at DE level and two records at MCE level (Kobe, 1995 and Manjil, 1987). Only one record (Kobe, 1995) exceeds the maximum downward vertical displacement band of 96.5 mm (3.80 in) defined for *PS2* at MCE level.

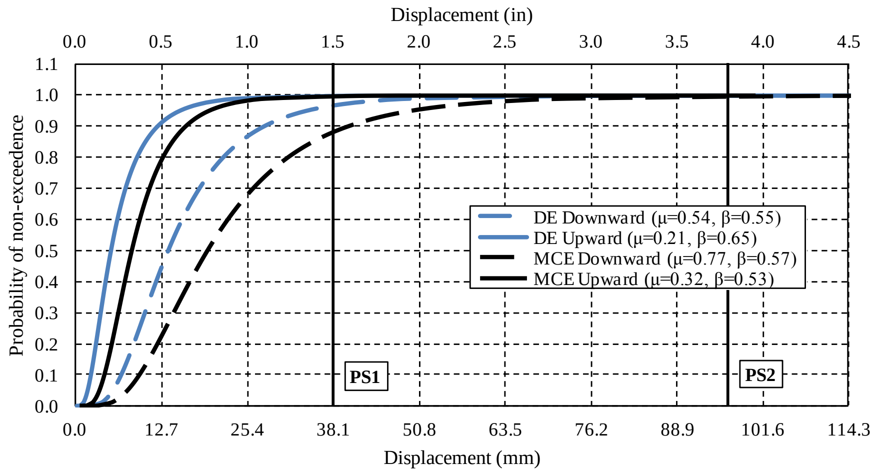

Figure 3.5. Cumulative probability plots of maximum downward and upward vertical displacements at mid-span

As described above, the contact zone between adjacent segments of the segmental superstructure is simulated by a set of compression-only contact springs. The axial deformations of the two springs, which are located at the top and bottom edges of the superstructure's cross-section, indicate the opening/closure of the joints when subjected to vertical earthquake loading. Figure 3.6 and 3.7 present the cumulative probability distribution functions of the deformations and strains measured at the top and bottom contact springs, located at the superstructure's mid-span, considering both DE and MCE seismic intensity levels. Also shown in Figure 3.7 are the two damage state bands listed in Table 3.1.

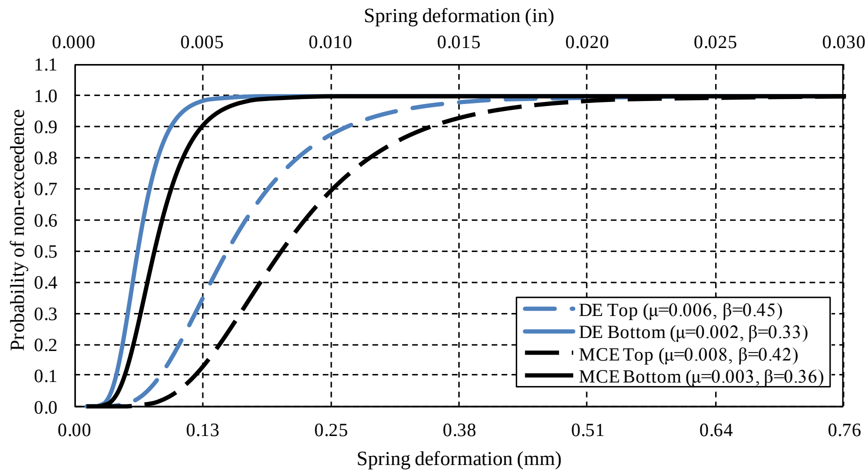

Figure 3.6. Cumulative probability plots of maximum top and bottom spring deformations at mid-span

Prior to loading, the mid-span superstructure joint is closed and the whole section is in compression. When a vertical seismic load is applied, the compression stresses increase on one side and decrease on the other side. Consequently, as the gap opening increases the neutral axis moves further inside the section. Based on Figures 3.5 and 3.6, the higher values of maximum downward displacement at mid-span are associated with high joint deformations at the top of the cross-section. The maximum compressive deformation at the top of the cross-section is equal to 0.56 mm (0.022 in) for the MCE level and is equivalent to a concrete strain of 0.12%.

According to Figure 3.7, the concrete compression strains developed at the bottom of the mid-span section are significantly lower than the strain band of 0.07% defined for *PS1* (see Table 3.1), for both DE and MCE intensity levels. On the other hand, the concrete compression strains developed at the top of the mid-span section have a probability of exceeding the strain band of 0.07% defined for *PS1* equal to 5% and 15% for the DE and MCE intensity levels, respectively. The strain band of 0.12%

defined for *PS2* is not exceeded for any of the considered cases. Therefore, higher joint deformations are expected at the top of the mid-span section but no significant damage or stiffness reduction is expected to occur.

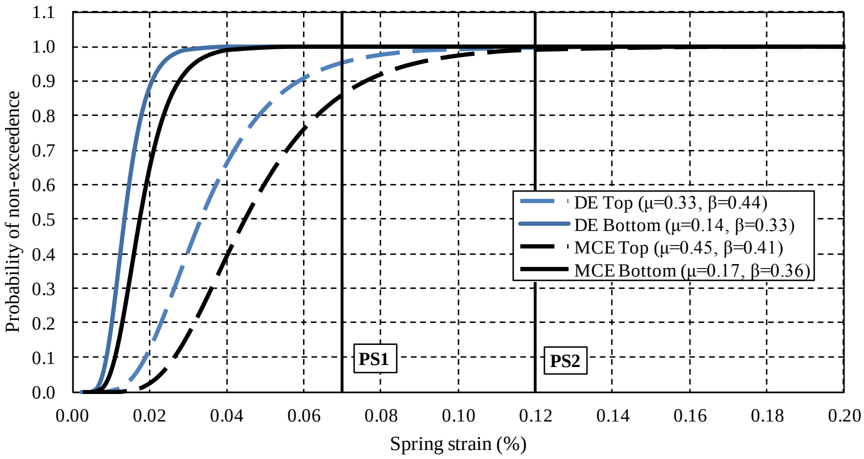

Figure 3.7. Cumulative probability plots of maximum top and bottom spring strains at mid-span

The rocking behaviour of the segmental superstructure is achieved through the restoring forces provided by the post-tensioning system. The stresses or strains developed by the unbonded tendons, which act as the continuous reinforcement between the superstructure's segments, are associated with the opening/closure of the segment-to-segment joints. Figure 3.8a presents the cumulative probability distribution functions of the axial tendon strain considering both the DE and MCE seismic intensity levels. The maximum strain value observed is equal to 0.62% for the MCE event. The results indicate that tendons remained in their elastic range, given that the tendon strain at yield is equal to 0.85% (see Table 3.1). This can be attributed to the fact that service loads, and not seismic loads, typically dominate the design of a bridge superstructure.

Figure 3.8b presents the cumulative probability distribution functions of the vertical residual displacement at the superstructure mid-span considering both the DE and MCE seismic intensity levels. The majority of the results are lying below a band value equal to 0.51 mm (0.02 in) whereas; the maximum value observed is equal to 2.79 mm (0.11 in) for the MCE event. Based on these results, the residual response of the segmental superstructure appears to be negligible which demonstrates the enhanced self-centring capability of the system.

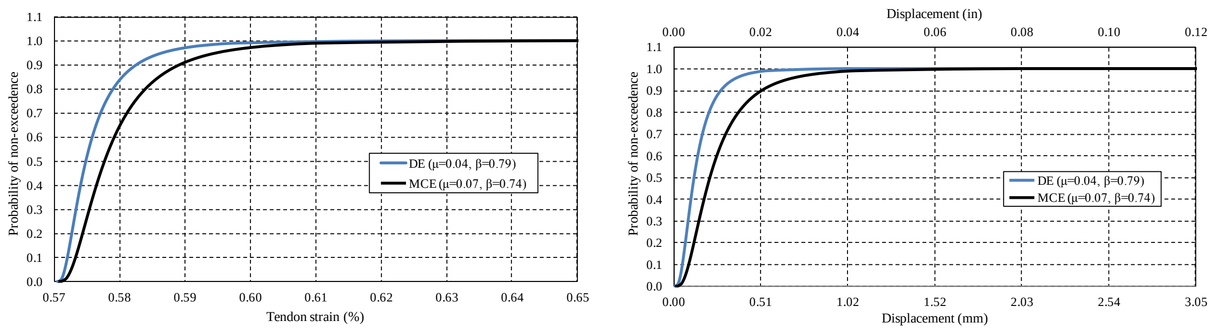

a) Tendon strain

b) Vertical residual displacement

Figure 3.8. Cumulative probability plots of tendon strain and vertical residual displacement at mid-span

4. CONCLUSIONS

This paper presents the results of a numerical study that investigates the response of a segmental concrete bridge superstructure when subjected to vertical earthquake motions. The proposed system, which uses internal unbonded tendons as the only continuous reinforcement along the bridge's length, is designed to exhibit high ductility and enhanced self-centring capabilities. The primary tool used in this investigation is a numerical model, which incorporates material and geometric nonlinearities, and is analysed under a set of multi-record Incremental Dynamic Analysis (IDA).

The IDA results, which focused on the response of the mid-span segment joint, showed that: the maximum downward displacements did not typically exceed the deflection limit specified by AASHTO (2007) for bridges under the effect of vehicular loads; the corresponding values of maximum upward displacement were significantly lower due to the geometry of the post-tensioning system; the joint opening remained way below the concrete spalling limit state minimizing the damage and stiffness reduction of the superstructure; the post-tensioning system remained in the elastic range and; the residual vertical displacements were negligible. These results demonstrate the satisfactory performance of the proposed segmental superstructure system with internal unbonded tendons, and prove its enhanced self-centring capabilities.

In this study, the IDA were terminated at an intensity level equal to the Maximum Considered Earthquake (MCE) level for a bridge site located in the Western United States. In order to verify the applicability of the recommended performance limit states, the model shall be subjected to higher seismic intensity levels that may result to its dynamic instability. Finally, this study indicates that vertical earthquake motions can significantly contribute to the joint response of segmental superstructures and therefore, they should be considered in the design process.

AKCNOWLEDGEMENT

Financial support for this research was provided in part by the Structural Engineering and Earthquake Simulation Laboratory (SEESL), Department of Civil, Structural and Environmental Engineering, State University of New York at Buffalo.

REFERENCES

AASHTO (2007). AASHTO LRFD Bridge Design Specifications, Americn Association off state Highway and Transportation Officials, Washington, D.C., United States.

Anagnostopoulou, M. (2009). Seismic Design and Analysis of Precast Segmental Concrete Bridge Superstructure, Master Dissertation, Centre for Post-Graduate Training and Research in Earthquake Engineering and Engineering Seismology (ROSE School), University of Pavia, Italy.

ASCE/SEI (2005). Minimum Design Loads for Buildings and Other Structures, ASCE/SEI 7-05, American Society of Civil Engineers, United States.

Carr, A.J. (2007). RUAUMOKO – Inelastic Dynamic Analysis, Department of Civil Engineering, University of Cantebury, Christchurch, New Zealand.

DYWIDAG-SYSTEMS INTERNATIONAL (2009). DYWIDAG Mono-strand Post-Tensioning System, DYWIDAG-Systems International, Illinois, United States.

FEMA (2009). Quantification of Building Seismic Performance Factors, FEMA P-695, Applied Technology Council for the Federal Emergency Management Agency, Washington, D.C., United States.

Megally, S.H., Garg, M., Seible, F., Dowell, R.K. (2002). Seismic Performance of Precast Segmental Bridge Superstructures, Structural Systems Research Project SSRP 2001/24, University of California at San Diego, La Jolla, California, United States.

Ou, Y. C., Tsai, M. S., Chang, K. C., Lee, G. C. (2010). Cyclic behavior of precast segmental concrete bridge columns with high performance or conventional steel reinforcing bars as energy dissipation bars. *Earthquake Engineering and Structural Dynamics*. **39:11**, 1181-1198.

Vamvatsikos, D. and Cornell, C.A. (2002). Incremental dynamic analysis. *Earthquake Engineering and Structural Dynamics*. **31**, 491-514.